c.

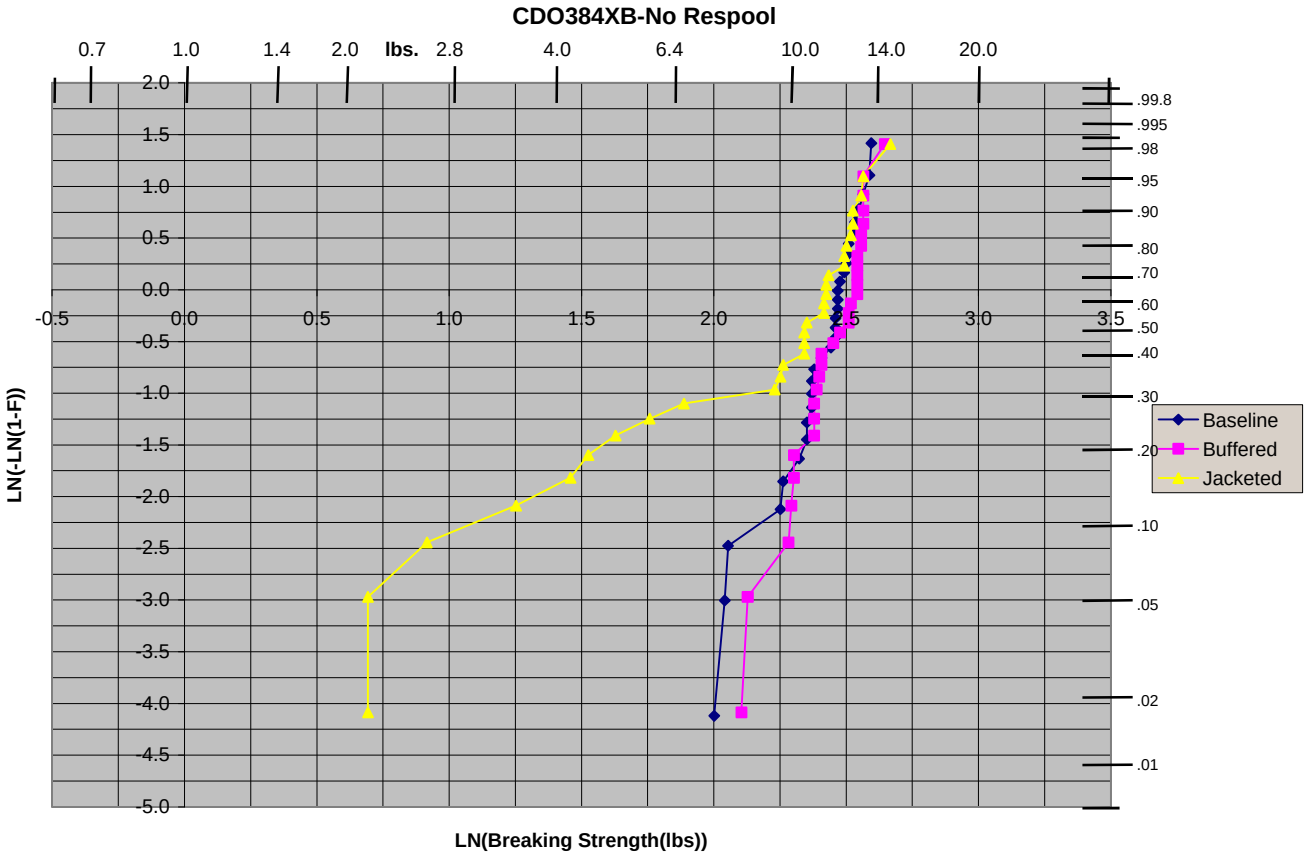
CDO384XB-No Respool
0.7
1.0
1.4
2.0
lbs.
2.8
4.0
6.4
10.0
14.0
20.0
2.0
1.5
1.0
0.5
0.0
-0.5
-1.0
-1.5
-2.0
-2.5
-3.0
-3.5
-4.0
-4.5
-5.0
-0.5
0.0
0.5
1.0
1.5
2.0
2.5
3.0
3.5
.99.8
.995
.98
.95
.90
.80
.70
.60
.50
.40
.30
.20
.10
.05
.02
.01
LN(-LN(1-F))
LN(Breaking Strength(lbs))
Baseline
Buffered
Jacketed

d.

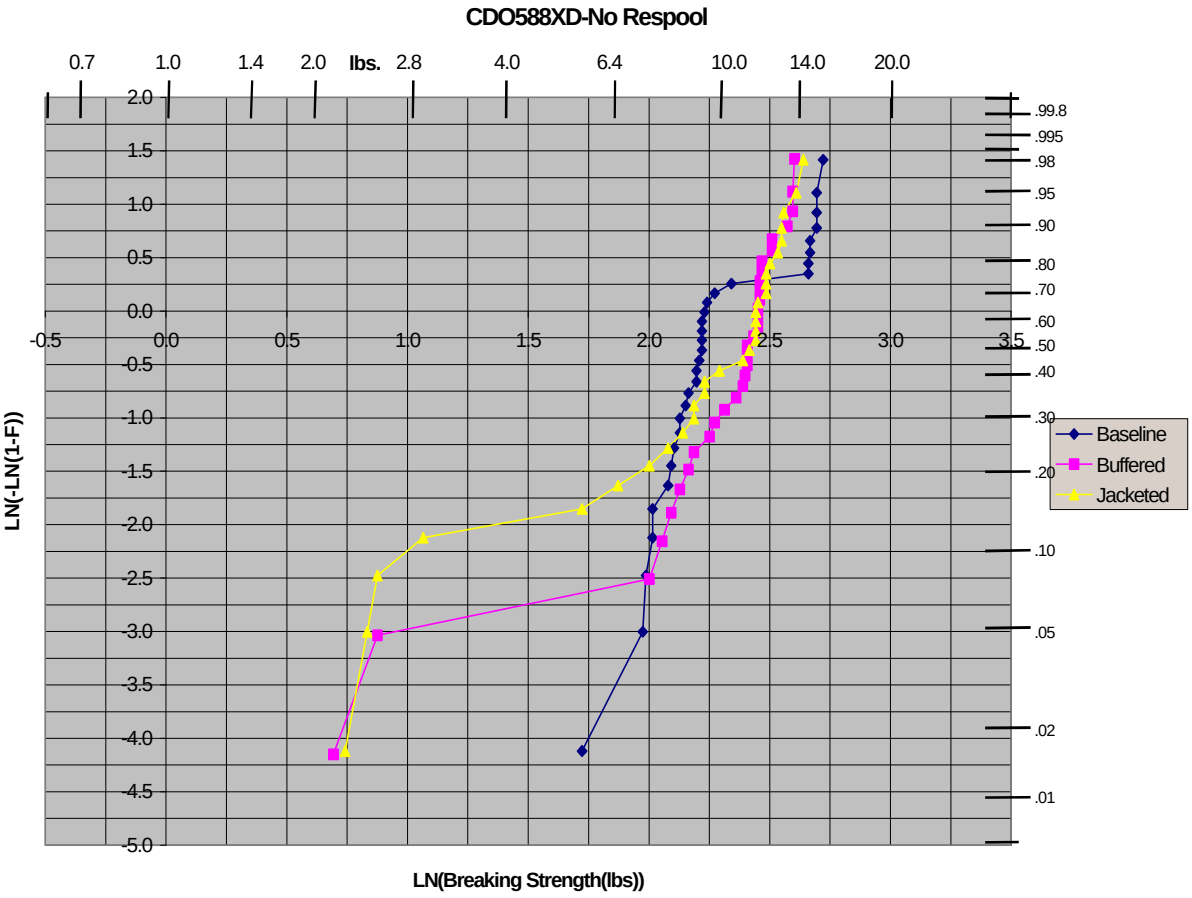

Figure 32 Strengths of DC0384 and DC0588 Fiber During Cabling

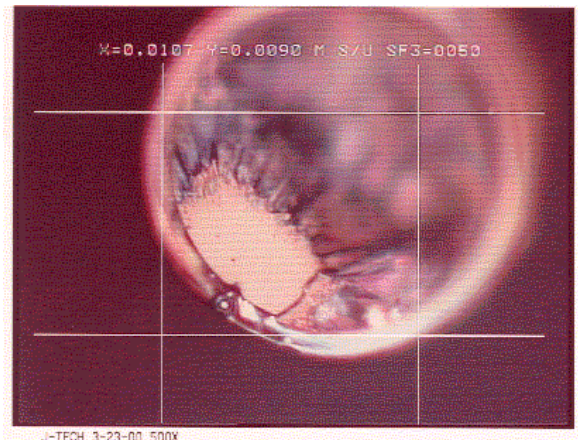

a. Stationary Fixture End, Fiber CD0588XCB, CD0588XCB, Sample 11

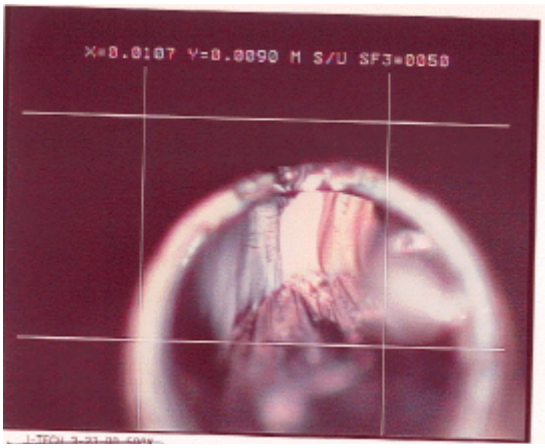

b. Moving Fixture End, Fiber Sample 11

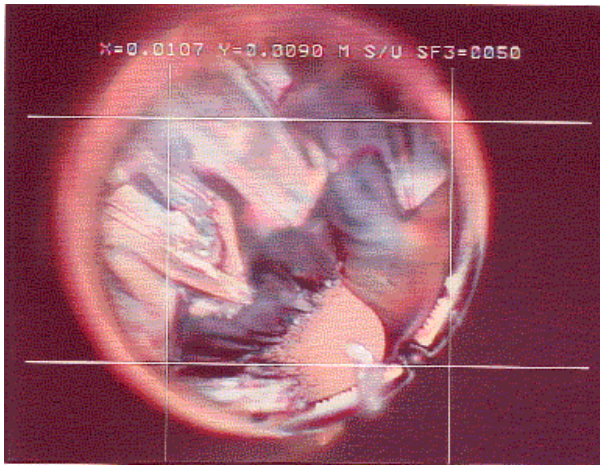

c. Stationary Fixture End, CD0588XCB, Buffered, Sample 11

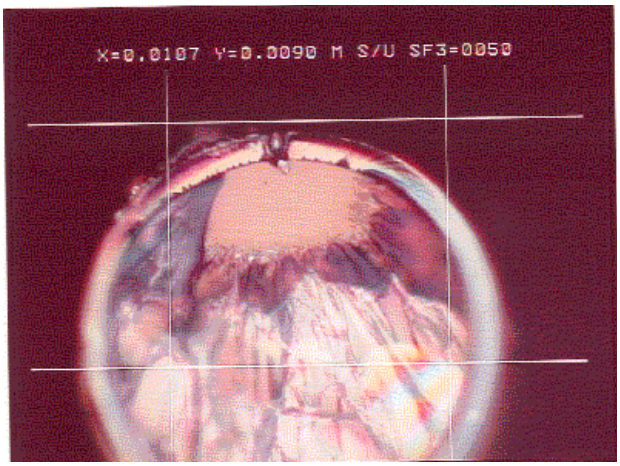

d. Moving Fixture End, Fiber, CD0588XCB, Buffered, Sample 11

Figure 33 Example of Low Strength Breaks

Figure 32a through 32d show that the fiber starts the process with high strength and every process step seems to weaken it, including the respooling process. They also show that the 588 fiber lot experienced greater weakening due to the cabling process that the 384 lot did, though they started with similar baseline strength. More bubbles were found in the polyimide coating during DPA on the 588 samples than on the 384 samples leading to continued interest in the correlation between the presence of the bubbles and latent defect sites.

Exposure to HF was used to try to measure the increase in etch related defects due to the respool and buffering cabling processes. Table 10 shows the results of this testing. The results point again to the propensity of the 588 lot to allow etch related defects versus the 384 lot. The 384 lot in this test, appears to be more robust with respect to defect creation or exacerbation associated with the respooling process. Figures 34a and 34b show the optical throughput during the etching period. [ref-25]

Table 10 HF Etch Results

Run #	Sample ID	Condition	Monitor wavelength	Total time	Time to change	#Breaks	#Scatters
			(nm)	hr:min	min		
1	CDO588XBRS#1	after respool	632.8	0:48	0:44	7	14
2	CDO588XBRS#2	after respool	632.8	2:10	1:06	3	16
3	CDO384XCRS#1	after respool	632.8	2:53	0:35 to 0:39	0	2
4	CDO384XCRS#2	after respool	1310	2:55	NA	0	1
5	CDO384XCCP#1	before respool	1310	1:17	0:17	1	0
6	CDO384XCCP#2	before respool	1310	2:33	NA	0	0
7	CDO588XBCP#1	before respool	1310	2:02	NA	1	0
8	CDO588XBBF#1	after buffer, in tube	1310	2:40	NA	0	0
9	CDO588XBBF#2	after buffer, removed from tube	1310	1:29	0:45	3	34
10	CDO384XCBF#1	after buffer, removed from tube	1310	2:22	1st 0:11	0	2
					2nd 1:30		

In all cases approximately 8 meters of fiber was subjected to HF vapor; approximately 1.5 to 2 meters was required to attach to monitoring equipment

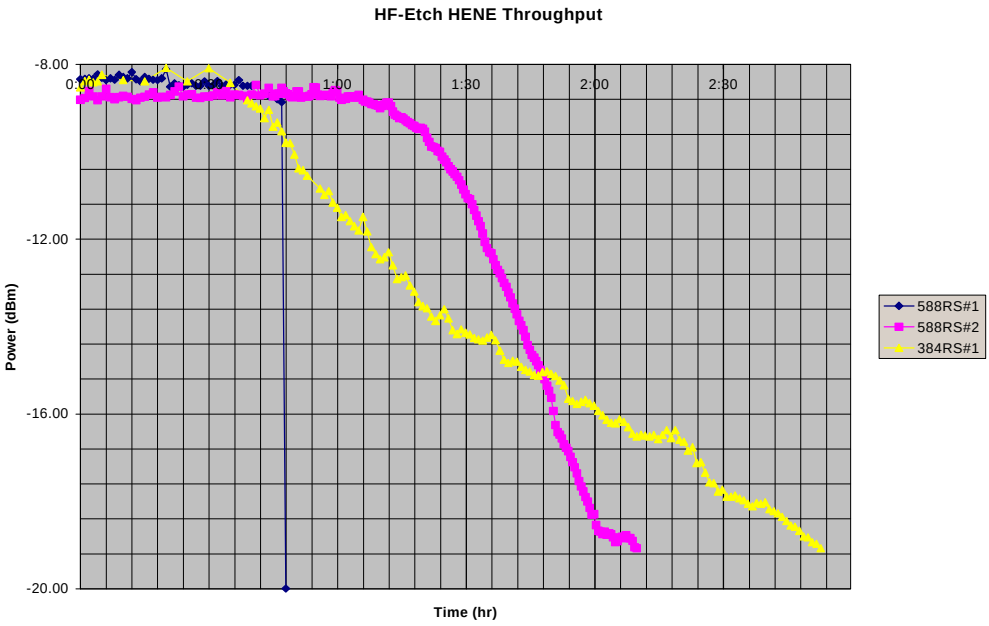

a. Run 1 through 3 with a HeNe source

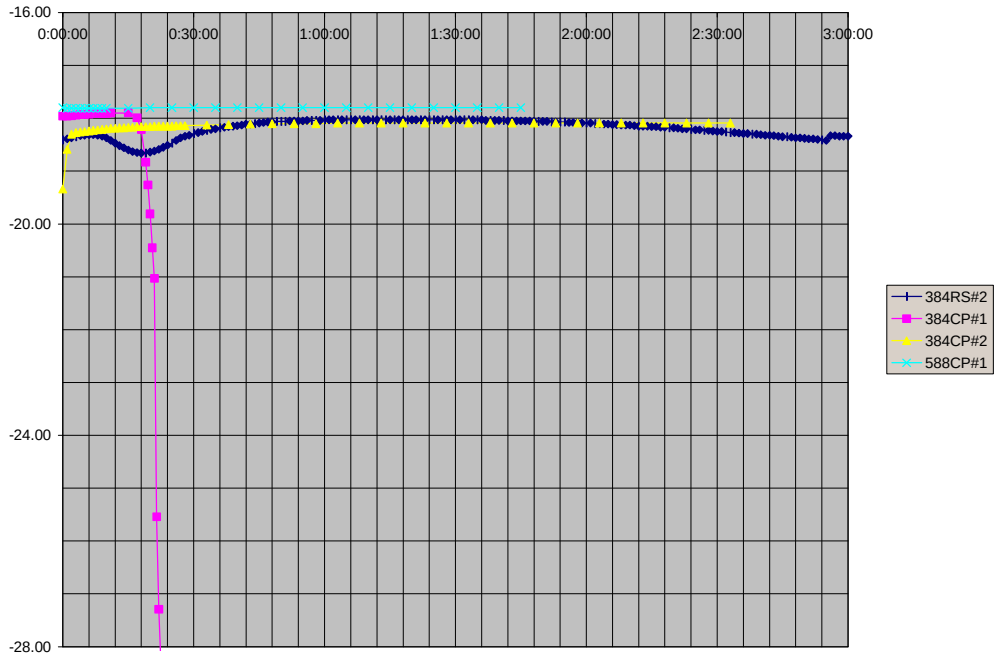

b. Run 4 through 7 with an 1030 LED source

Figure 34 Optical Throughput During HF Etch Test

7.3 Strength Testing Non-Carbon Coated Fiber

A third round of testing was performed to see if the weakening of the fiber due to the respooling process was unique to the carbon coated fiber. Table 11 shows the test plan used.

Table 11 Test Plan for Strength Testing of Non-Carbon Coated Fiber

Sequence #	Operation or Test	Length used (m)	Facility	CDO384XB	CDO588XD	CDO858XB1	CDO731XB
	Starting Sample Lengths			1847	918	2200	2200
1	OTDR/Visible Fault location	NA	BICC			2200	2200
2	Loss (1300 nm)	1	BICC			2199	2170
3	Retain Top of Spool Individual Control Sample	50	BICC			2149	2120
4	Baseline Dynamic Tensile Strength Samples	30	BICC			2119	2090
5	Baseline HF-Etch Samples	30	BICC			2089	2060
6	Retain Top of Spool Individual Control Sample	50	BHB	1797	868		
7	Baseline Dynamic Tensile Strength Samples	30	BHB	1767	838		
8	Baseline HF-Etch Samples	30	BHB	1737	808		
9	Respool/LaserMike™/Current & Field Probe	150	BICC	1587	658		
10	Respool/LaserMike™/Current & Field Probe	600	BICC			1489	1460
11	OTDR/Visible Fault location	0	BICC			1489	1460
12	Remove Dynamic Tensile Strength samples	30	BICC				
13	Remove HF-etch samples	30	BICC				
14	Extrude loose tube buffer	540	BICC	1047	118	949	920
15	Retain End of Section Individual Control Sample	50	BICC	997	68	899	870
16	Remove EOS Dynamic Tensile Strength Samples	30	BICC	967	38	869	840
17	Remove End of Section HF-Etch Samples	30	BICC	937	8	839	810
18	Remove excess fiber from process account			0	0	0	0
19	Extrude loose tube buffer	40	BICC				
20	Insert Buffered fibers (step 14) into remaining steps			500	500	500	500
21	OTDR/Visible Fault location	0	BICC	500	500	500	500
22	Remove Dynamic Tensile Strength samples	30	BICC	470	470	470	470
23	Remove HF-etch samples	30	BICC	440	440	440	440
24	Apply strength member	0	BICC	440	440	440	440
25	OTDR/Visible Fault location	0	BICC	440	440	440	440
26	Remove Dynamic Tensile Strength samples	30	BICC	410	410	410	410
27	Remove HF-etch samples	30	BICC	380	380	380	380
28	Extrude Jacket	40	BICC	340	340	340	340
29	OTDR/Visible Fault location	0	BICC	340	340	340	340
30	Remove Dynamic Tensile Strength samples	30	BICC	310	310	310	310
31	Remove HF-etch samples	30	BICC	280	280	280	280
32	Complete Dynamic Strength Tests-Baseline Samples		BHB				
33	Complete HF-Etch Tests-Baseline Samples		BHB				
34	Complete Dynamic Strength Tests-Respool Samples		BHB				
35	Complete HF-Etch Tests-Respool Samples		BHB				

Table 11 Test Plan for Strength Testing of Non-Carbon Coated Fiber *(Cont'd)*

Sequence #	Operation or Test	Length used (m)	Facility	CDO384XB	CDO588XD	CDO858XB1	CDO731XB
36	Complete Dynamic Strength Tests-Braided Samples		BHB				
38	Complete Dynamic Strength Tests-Jacketed Samples		BHB				
39	Complete HF-Etch Tests-Jacketed Samples		BHB				
40	Complete Dynamic Strength Tests-EOS Samples		BHB				
41	Complete HF-Etch Tests-End of Section Samples		BHB				
	Virgin Fiber Left at end of tests			937	8	839	810

The fiber from the non-carbon coated lots, CD0858XB1 and CD0731XB are polyimide coated but do not have the carbon under-layer. The Lucent-SFT product number for this fiber is BF04455. The preform is SG320, not the rad-tolerant "320R" type used in the preform used to make BF04515 fiber.

7.3.1 Results: Strength Testing Non-Carbon Coated Fiber

Figure 35a through 35c show the affect of the various cabling processes on the fiber strength for the non-carbon-coated fibers. The unprocessed fiber has high strength, however as it goes through cabling, its strength is again increasingly reduced. The difference in the behavior between the two non-carbon coated fiber lots is still under study. [ref-26]

a.

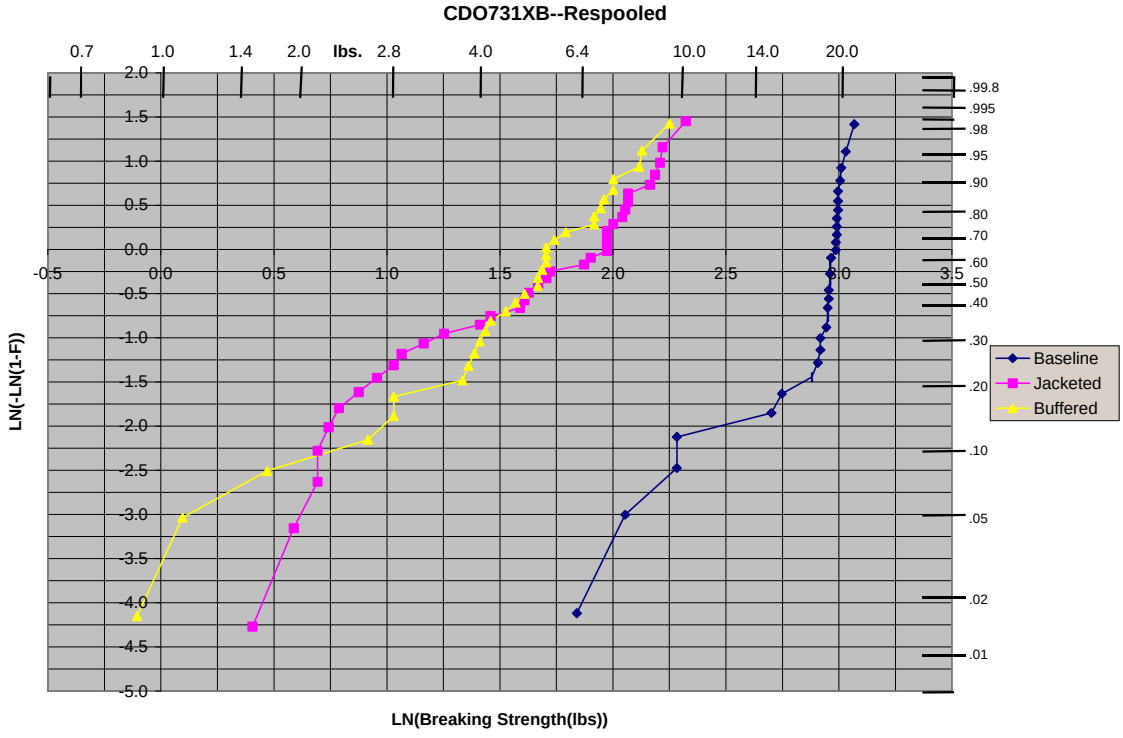

b.

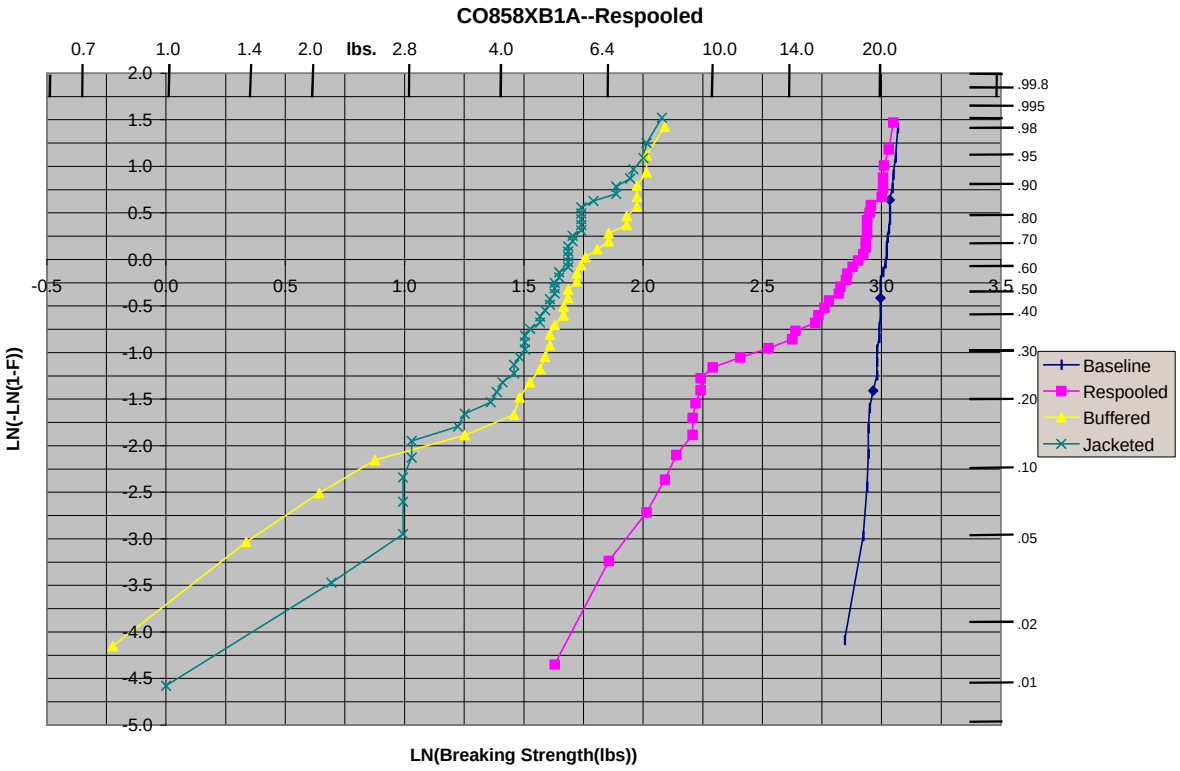
CO858XB1A--Respooled
0.7
1.0
1.4
2.0
lbs.
2.8
4.0
6.4
10.0
14.0
20.0
2.0
1.5
1.0
0.5
0.0
-0.5
-1.0
-1.5
-2.0
-2.5
-3.0
-3.5
-4.0
-4.5
-5.0
-0.5
0.0
0.5
1.0
1.5
2.0
2.5
3.0
3.5
.99.8
.995
.98
.95
.90
.80
.70
.60
.50
.40
.30
.20
.10
.05
.02
.01
LN(-LN(1-F))
LN(Breaking Strength(lbs))
Baseline
Respooled
Buffered
Jacketed

c.

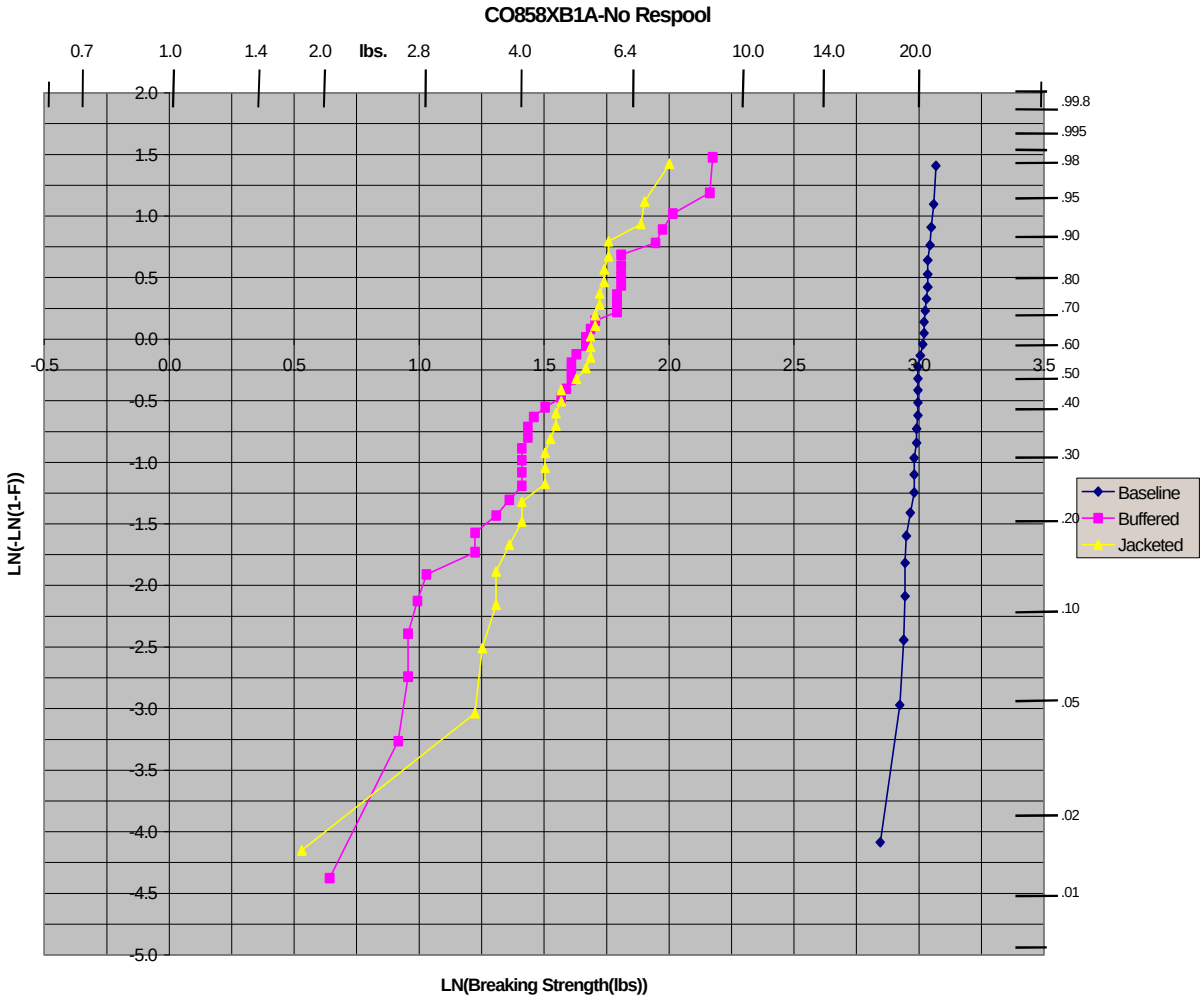

Figures 35 Strength for the Non-carbon Coated Fibers

7.4 Mandrel Test Screening of Cabled Fiber

Testing was performed to determine if a mandrel proof test could be performed as an incoming screen to remove low strength fiber. Figure 36a and 36b shows the mandrel arrangements and sizes used. Lengths from cable lot 04245 and 04255 had been strength tested as discussed in section 7.1 above. The 04245 lot was found to contain more low strength sites than 04250 though the 04250 lot also had similarly weak links. Both of the samples were screened for glows with a HeNe laser and for echoes with an OTDR. This established that the 04245 sample was starting the evaluation with at least one flaw. No glows were found for the 04250 sample and no echoes were found for either. The samples were then submitted to the proof test, which extended roughly 100 kpsi (2.4 lbs) to the cable.

The fracture surfaces of the breaks found in the 04250 sample were analyzed and breaking strengths in lbs were calculated for them. These have been superimposed on the curve of breaking strengths found for the surviving sample, which was strength tested after the mandrel wrap screen. The lower (blue) section of Figure 37 represents the calculated values. The blue portion of the curve in Figure 38 are extrapolated values for the breaks, which occurred during the mandrel wrap screen in the 04245 sample. Figure 39 shows the dynamic strength data alone.

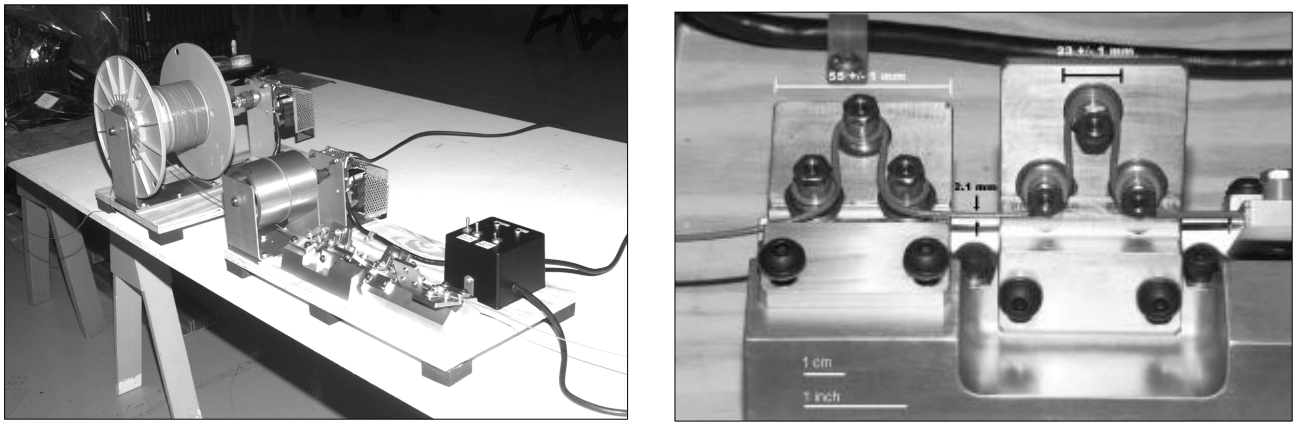

a. *b.*

Figure 36 Mandrel arrangements and Sizes Used

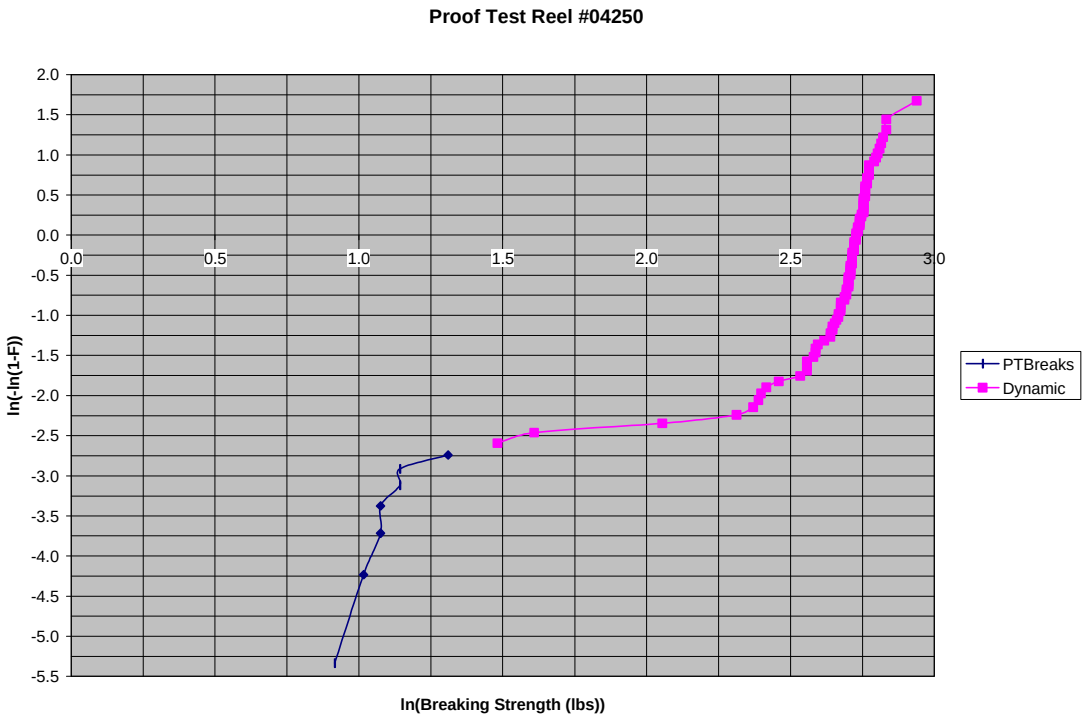

Figure 37 Hypothetical Break Strengths During Screen Compared to Actual Break Strengths on Proof Test Screened Sample

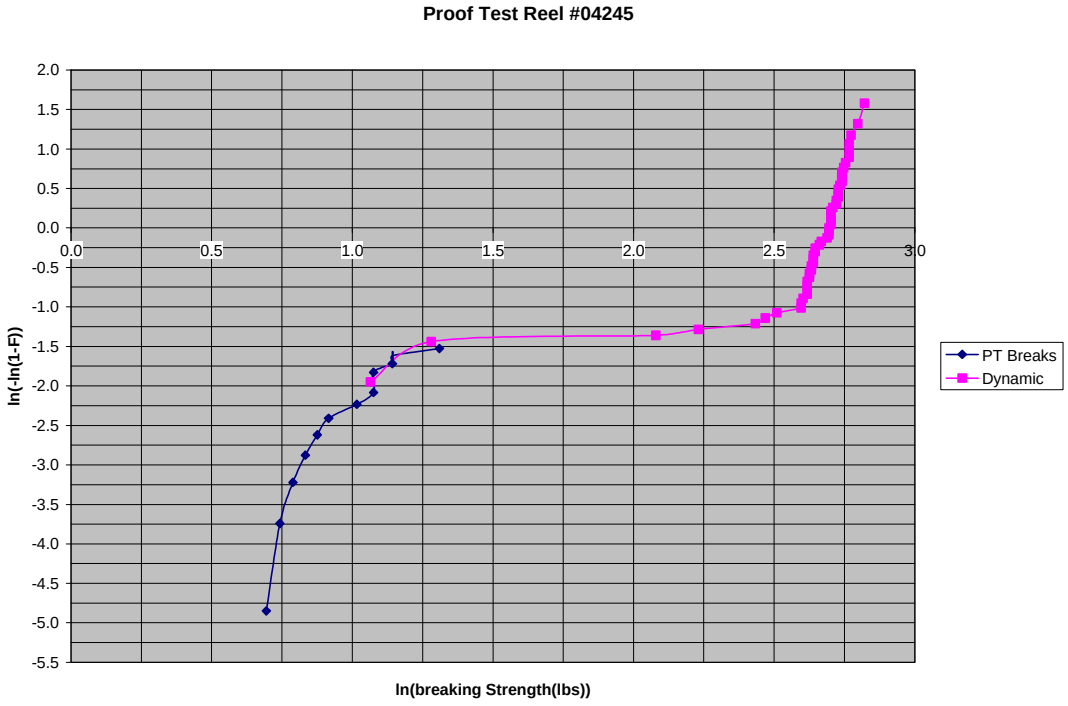

Figure 38 Mandrel Used for Screening Evaluation

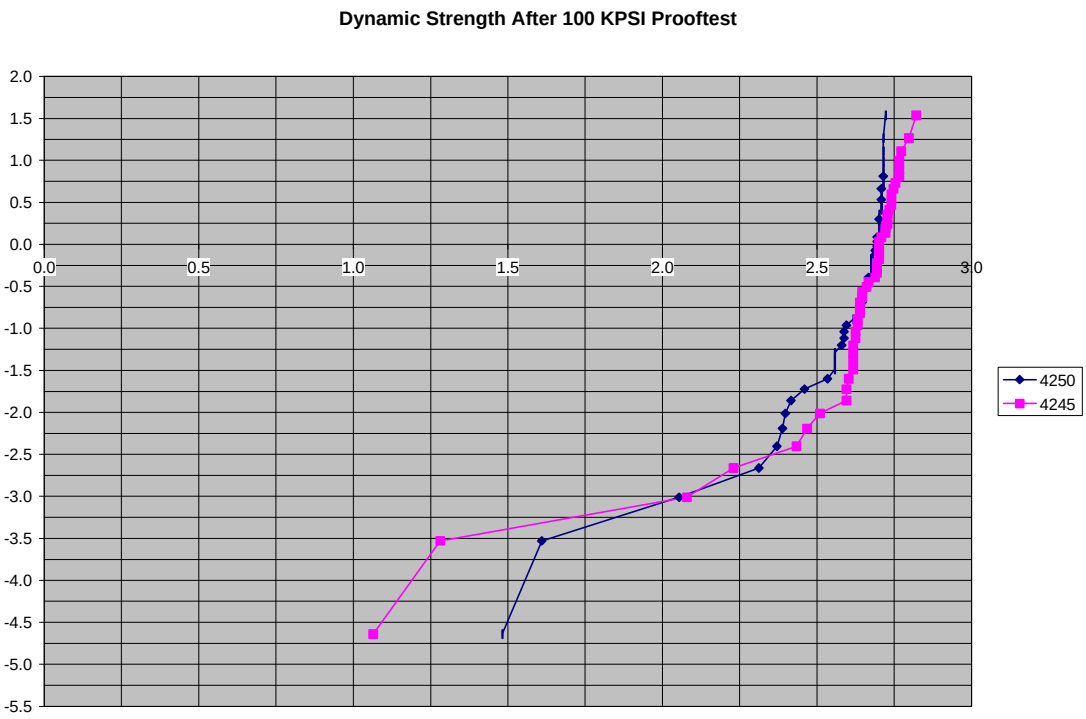

Figure 39 Dynamic Strength Data for the Pre-Proof Test Screened Cables

8.0 CONCLUSIONS

The cable design which has been associated with “rocket engine” defects, within the optical fiber, and later with low breaking strengths of the fiber, has been that defined by the ISS specification SSQ21654 (plus engineering modifications) and given the Boeing Company part number NFOC-2FFF-1GRP-1. Some small amounts of a similar part number, NFOC-2TFF-1GRP-1 was also used in ISS hardware; however, the problem investigation reported here does not concern this second part number. The production period of concern spans between June of 1996 to July of 1999. End users were Boeing-HB, ISS partners, and their subcontractors.

The fiber and cable build history indicates only two major process changes over the period in which the NFOC-2FFF-1GRP-1 was made; (1) use of different draw towers at different plants of the fiber manufacturer, and (2) implementation of a respooling operation at the cabling plant. Upon initial review, the available traceability data did not conclusively indicate that these process changes were the sole cause of the “rocket engine” defect. The investigation has brought into light a better understanding of the latency of the defects, warranting another review of the traceability data for pointers to weaker cable lots.

The manufacturing process review identified several processes that contribute to the creation of “rocket engine” defects and of fiber strength reducing defects. Though none of the processes used are outside of normal practice for making specialty fiber or cable, they become uniquely undesirable for this cable because of the materials involved in this cable design.

The conditions present in the cabling processes, specifically with respect to the behavior of FEP at the temperature at which it is extruded while surrounded by air, create carbonal difluoride (COF_2). Carbonal Difluoride reacts with water resident in the polyimide to create hydrogen fluoride (HF) which etches the glass fiber wherever it is not covered by the carbon coating. The “rocket engine” defect is the result of HF etching, the products of which can be found in and around the etch pit and which are silica balls and germania crystals.

The root cause for the breaches in the carbon coating is still not understood well enough to predict the frequency of their occurrence. These breaches have been found to be 1 to 3 μm in size, and are often in the vicinity or directly below a distinct feature in the polyimide coating. This size makes them invisible to a screen, which uses electrical resistance as a measure of coating quality. The size may also make hydrogen ingression, and proof testing, incapable of identifying fiber that contains breaches at the rate of one per millimeter, or less. No practical screening method has been found which can be used to find these carbon breaches.

The polyimide features which accompany the “rocket engine” defects and low strength breaks have been found in at least three configurations: cups, buried voids (bubbles) and thinned areas (sink holes). Surface blisters are not being considered in this investigation. Data book values cannot be used to predict how the polyimide will perform mechanically and electrically because the polyimide is applied to the fiber in a way that differs substantially from the convention preparation of polyimide. Testing showed that the polyimide will break down at voltages between 3.5 kV and 4.0 kV where the features are not present, and at as little as 1.5 kV where thinning exists because of the presence of a feature. We believe that ESD events will be focused at the polyimide features because they reduce the dielectric’s thickness from 15 μm to as little as several micrometers. Though geometric analyses of the static fields measured around the fiber during fiber and cable manufacturing (specifically around the proof test during fiber manufacture and during respooling during cable manufacture) have not been done, it is believed that the actual potentials at the fiber surface during those processes are sufficiently high to support discharge events through the polyimide coating at these features. Testing showed that high current discharges will damage the polyimide severely and the carbon as well. It is believed that lower current events, which may not result in observable damage to the polyimide, are causing breaches in the carbon coating and the glass below it.

The co-location of the polyimide features and the carbon breaches has been shown; however, the preference for etching at some carbon breaches and not at others has not been explained. Periodicity has been seen with respect to the distribution of the etch sites and with respect to the distribution of the polyimide features. A better understanding of this periodicity may point to the process sources of the polyimide features and the carbon breaches.

Many screening and analysis methods were used in the study of this problem; some were successful and some others were not. Optical performance methods such as the use of commercial optical fault finders (OFF; 1 mW power) and specialty fault finders (OFF using 20 mW to 30 mW) tended to be more easily and successfully applied than the various OTDR's that are available. The farther the etch pit reached into the core, the more effective the OFF and OTDR screen was. Optical power meters were similarly useful: these detect deep etch pits. All three were not useful as a screening method when a shallow crack occurred in the exposed glass at a carbon breach (which reduces the fiber's life), but no etch pit removing waveguide material was present, which would effect the light throughput. In-line laser micrometers were not able to detect the polyimide surface features that indicate a fiber which contains latent defects. An IR laser based system may be useful in this way; however, more investigation will be required. Mandrel wrap screening gave promising results in its ability to screen low strength breaks from cabled fiber.

SEM and optical microscopy were very useful in DPA analyses. The use of index matching fluid was very useful for optical microscope inspection. X-ray has limited applicability with respect to fiber surface features however it is useful for understanding the configuration of fiber breaks still inside of the cable.

Strength testing has demonstrated the initial high strength of the fiber, even with the presence of what are believed to be latent defects. Prior study of carbon coated glass has shown it to have high strength over a wide range of strain rates. The Weibull plots of the breaking strength data for the respooled, partially cabled, and cabled fiber (using processes defined for NFOC-2FFF-1GRP-1) show that those cabling operations and other ancillary processes, including handling, introduce a population of low strength breaks into the BFO4515 fiber. The fiber was found to break with a distribution tail normally associated with non-hermetic glass whose surface defects are growing into cracks with handling stress. Non-hermetic fiber was tested throughout the cabling process as well and similar results were found.

Conventional n-theory-based life predictions could not be made using the dynamic fatigue data collected because it did not follow the basic laws of that theory. It is believed that one reason is that multiple failure modes were occurring in the fiber that was tested. Fiber life predicting using n-theory is designed for fiber whose only failure mode is crack propagation due to strain rate. It may not be impossible to develop similar predictive theory for the NFOC-2FFF-1GRP-1 system; however, it was outside of the scope of this investigation to accomplish that task.

9.0 RECOMMENDATIONS

The initial goal of this investigation was to understand the cause of the "rocket engine" defects found in the fiber contained in the NFOC-2FFF-1GRP-1 optical cable being used by Boeing in International Space Station hardware. It was believed that if the root cause of the rocket engine defect could be found, the handling or the manufacturing processes (or both) could be engineered to eliminate the defect from future hardware. As the investigation progressed, these defects began to be understood as distinct and related to synergistic processes occurring during fiber and cable manufacturing. While interest continued in tracking down the root causes of what was now a collection of defects, additional approaches to the problem resolution were explored. They included using screening to eliminate the defects from the product used to build flight hardware, and risk assessment to understand what level of defects may be tolerable given the reliability requirements established for ISS and the installation conditions used.

9.1 Processes Which Create Defects

It has been established that the cabling process being used to make the NFOC-2FFF-1GRP-1 cable, using the BF04515 fiber, will create COF_2 and ultimately HF. Processing FEP under dry nitrogen (to remove oxygen), during FEP processing and eliminating the water in the polyimide coating during buffer extrusion, will reduce the volume of HF produced during cabling by several orders of magnitude.

Breaches in the carbon on the fiber allow HF etching and strength reduction of the glass fiber. Direct inspections have shown the frequency of the etch pits varies widely along a given fiber and also varies between different fiber runs. More study of the carbon layer through materials analysis could provide insight into why this is so.

The frequency of polyimide features is also variable with the fiber draw lot. Their connection with carbon breaches and exposure of the fiber to ESD events of a lower strength than that afforded by a continuous, uniformly thick layer, indicates that they too should be eliminated. More study in many areas, including materials analyses and electrical and mechanical environmental analyses, is required to understand how the bubbles are formed. The development of successful screening methods for both carbon defects and the polyimide features will greatly contribute to understanding when the defects are occurring, as well as supporting the removal of these defects.

9.2 Screening Methods

The transparency of the fiber and its polyimide coating, and the fiber's geometry (especially its cylindrical shape and aspect ratio which is on the order of 10^9 to 10^{10}) make it extremely challenging to inspect. Screens, which can detect polyimide features, now associated with carbon breaches, should be developed to eliminate known latent defects. A similar screen for carbon breaches would be critically useful.

Dynamic strength testing should be used as part of a qualification; also, this testing should be repeated on some schedule. Development of the madrel wrap test should continued through repeatability and validation testing so that it can be demonstrated to be a non-destructive, 100% screen. Standardization of the test method through the EIA/TIA is also recommended. Future specification documents should use these tests to qualify and screen flight lots.

Lessons were learned during the investigation about improvements that could be made to the procurement specifications. Several improvements can be made with respect to specific definitions for fiber and cable production lots. Traceability of all finished cable harnesses back to all raw material lots and the fiber lot should be required. The fiber should be qualified by the end user and the cable specification should require use of qualified fiber in its construction (reference MIL-PRF-27500 for cable, which requires the use of MIL-PRF-22759 wire). The fiber lot should be defined and traceable back to the preform. The fiber and cable specifications should contain: lot-based screening (non-destructive, 100% basis, "Group A"), lot-based inspections (non-destructive and destructive mechanical and environmental tests, sample basis, every lot, "Group B" tests) and periodic qualification tests (destructive and non-destructive mechanical and environment tests and reliability validation, schedule based on production schedule, "Group C" tests). Self-auditing by the user should be used to confirm that the traceability requirements are being met.

The new failure modes associated with the etch pits and low strength will need to be addressed in the new specification. As new screens become available, as recommended above, they should be added to the specification.

9.3 Reducing Risks Associated with NFOC-2FFF-1GRP-1 Cable

Logistical and budget pressures will force the use in flight hardware of product produced by the same processes which created the latent defects and failures discussed in this report. Measures can be taken to reduce some of the risks associated with this cable stock. It has been established that the cable has an ESD sensitivity. This report states that a threshold of 1.5 kV was measured although that value could be less depending on the thinness of the polyimide at a defect site. More work could be done to further quantify the ESD sensitivity of this cable and to establish handling and installation requirements, which will protect the cable from ESD damage. It is strongly recommended that cablers and manufacturers of carbon coated fiber measure the electrostatic conditions in their plants and make modifications to equipment and handling processes which can introduce discharge events involving the fiber.

Any stress reduction that can be obtained by modifications to the installation plans for future builds will extend the life of this cable. Opportunities may exist for reducing stress on the cables when in-flight repairs are made where vibration conditions don't have to be accounted for (open supports rather than tie-downs can be used).

Finally, in order to gain insight about the rate at which the links are expected to break in flight, a static fatigue test (hanging weights from lengths of fiber in an environment at fixed temperature and humidity) should be performed.

10.0 REFERENCES

[ref-1: email: 3/20/00, From: William Weisenberger, "U.S. Lab ROM for Bending of Fiber"]
[ref-2: email: From: Ray Prestridge, RE: Fiber Optice, Attachment: SSQ_21654RB.PDF]
[ref-3: email: Ray Prestridge, "Words for 'PFA in ISS Node 1' paragraph", 7/23/00]
[ref-4: email: Henning Leidecker, "Fwd: RE: Fwd[2]:latest pictures", 11/12/99]
[ref-5: email: Brad Cothran, Boeing-KSC, "RE: Acceptance limit for finished harnesses", 3/14/00]
[ref-6: email: Dale Zevotek, "RE: OTDR that you use", Attachment: OC-1614.tif, 2/24/00]
[ref-7: Reference Manual, Model OFM, Optical Fiber Monitor, Opto-Electronics Inc., 1996]
[ref-8: C.T. Mueller and J.G. Coffer, "Polyimide/Carbon Defects", The Aerospace Corporation, 6/21/00]
[ref 9: Teflon Mechanical Design Data, Du Pont Company, no date]
[ref 10: Guide to the Safe Handling of Fluoropolymer Resins, The Society of the Plastics Industry, Inc., 1998]
[ref 11: Thermal degradation of commercial fluoropolymers in air, Bertsil B. Baker, Jr., Daniel J. Kasprzak, Polymer Degradation and Stability 42, 1993]
[ref-12: http://hdmicrosystems.com/2produts/prodlist.html]
[ref 13: The Nature of Water Absorbed by Polymeric Electronic Packaging Materials, Brian Dickens, G.T. Davis, http://www.nist.gov/msel/div854/electapps/1995_projects/nature3.html]
[ref 14: Moisture Effects in Electronic Packaging Polymers, no author, http://www.nist.gov/msel/div854/electapps/1996_projects/moisture2.html]
[ref 15: C.T.Mueller, J.G. Coffer, and T. Giants, "ISS Fiber Status", The Aerospace Corporation, 3/9/00]
[ref-16: email: D. DiGiovanni , "Re: Fw: Anyone have Jay Lee's new email address?", Lucent-Bell Laboratories, 4/26/00]
[ref-17: Eric A. Lindholm, Jie Li, Adam S. Hokansson, and Jaroslaw Abromczyk, Spectran Specialty Optics Company, and Sara E. Arthur, David R. Tallant, Sandia National laboratories, "Low Speed Carbon Deposition Process for Hermetic Optical Fibers", "International Wire and Cable Symposium, 1999".]
[ref-18: email: Craig Mueller, "Charts showing Carbon Pinhole and Bubble Defect Shape", 07/05/00]
[ref-19: Mallock, Proceedings of the Royal Society, vol 9, page 262, 1907]
[ref-20: A.B. Wood, "A Textbook of Sound: being an account of the physics of vibrations with special reference to recent theoretical and technical developments", 1930]
[ref-21: email: Gary Bickel, "Detail Coating Penetration Test Plan and Schedule", 3/15/00, Attachment: CoatingTstPln.xls]

[ref-22: email: Gary Bickel, Boeing-HB, FiberB&A.xls>> <<CoatingTestData.xls>> <<Respool384.xls>>, 3/25/00><<Respool588.xls>>]
[ref-23: email: Gary Bickel, Coating Penetration Tests: Strength Test Results on CD0588XB, 4/4/00]
[ref-24: email: Gary Bickel, Coating Penetration Tests: Strength Test on CD0588XC, 4/4/00]
[ref-25: Gary Bickel, Strength and HF-Etch Tests, 4/7/00]
[ref-26: Gary Bickel, "Revised Non-carbon-coated test Results", 7/18/00]

11.0 ACKNOWLEDGEMENTS

The Team 2, Root Cause Investigation Team, gratefully acknowledges the contributions of the following individuals whose efforts made this work and this report possible:

Jerry Arnett, The Boeing Company
Marvin E. Banks Jr., Boeing M&P, Kennedy Space Center
Harold Battaglia, The Boeing Company
Dave Beverly, NASA GSFC
Dr. Gary Bickel, The Boeing Company
Dr. John Canham, Unisys Corporation
Anna Cantwell, SEA Wire and Cable
Brad Cothran, The Boeing Company
David Gill, The Boeing Company
John Kolasinski, NASA GSFC
Dr. Henning Leidecker, NASA GSFC
Jim Holt, US Army Aviation & Missile Command
Jie Li, Lucent Specialty Fiber Technologies
Eric Lindholm, Lucent Specialty Fiber Technologies
Billy-Jo Mitchell, BICCGeneral
Carmen Moore, The Boeing Company
Pete Mueggler, The Boeing Company
Dr. Craig Mueller, The Aerospace Corporation
Mike O'Conner, Lucent Specialty Fiber Technologies
Melanie Ott, Sigma Research
Chris Pegge, BICCGeneral
Jeannette Plante, Swales Aerospace
Ray Prestridge, Lockheed-Martin Corporation
Dave Rothermel, BICCGeneral
Martin Seifert, Lucent Specialty Fiber Technologies
John White, The Boeing Company
Dale Zevotek, BICCGeneral

Special Thanks are extended for report production assistance to:

Jesse Frank, Swales Aerospace
Silvia Romero, Swales Aerospace
Carl Szabo, Swales Aerspace

Special thanks are extended for ISS Fiber website maintenance to:

Jesse Frank, Swales Aerospace